Reprinted from
Jpn. J. Appl. Phys. Vol. 40 (2001) pp. 441–445
Part 1, No. 1, January 2001

Experimental Evaluation of Pencil Beam Algorithm by Measurements of Dose Distributions of Protons Traversing an L-Shaped Phantom

Ryosuke KOHNO, Yoshihisa TAKADA, Takeji SAKAE[1], Akihiro NOHTOMI, Toshiyuki TERUNUMA[2] and Kiyoshi YASUOKA[3]

Institute of Applied Physics, University of Tsukuba 305, Japan
[1]*Institute of Clinical Medicine, University of Tsukuba 305, Japan*
[2]*Proton Medical Research Center, University of Tsukuba 305-0801, Japan*
[3]*Institute of Basic Medical Sciences, University of Tsukuba 305, Japan*

Jpn. J. Appl. Phys. Vol. 40 (2001) pp. 441–445
Part 1, No. 1, January 2001

Experimental Evaluation of Pencil Beam Algorithm by Measurements of Dose Distributions of Protons Traversing an L-Shaped Phantom

Ryosuke KOHNO*, Yoshihisa TAKADA†, Takeji SAKAE[1], Akihiro NOHTOMI, Toshiyuki TERUNUMA[2] and Kiyoshi YASUOKA[3]

Institute of Applied Physics, University of Tsukuba 305, Japan
[1]*Institute of Clinical Medicine, University of Tsukuba 305, Japan*
[2]*Proton Medical Research Center, University of Tsukuba 305-0801, Japan*
[3]*Institute of Basic Medical Sciences, University of Tsukuba 305, Japan*

(Received August 18, 2000; accepted for publication October 23, 2000)

A proton dose-calculation method has been developed on the basis of the pencil-beam algorithm (PBA), which is expected to improve the precision of the conventional method based on the broad-beam algorithm (BBA). In order to verify the accuracy of calculation by the PBA, dose distributions formed by a horizontal proton beam traversing a phantom with an L-shaped horizontal cross section were measured using a silicon semiconductor detector (SSD) in a water vessel. The results of the measured dose distributions agree well with the ones calculated using the PBA within an rms error of 2.3%. Therefore, the dose-calculation method by the PBA is useful and applicable to actual treatment planning of the proton therapy.

KEYWORDS: proton, dose distribution, pencil-beam algorithm, broad-beam algorithm, silicon semiconductor detector

1. Introduction

We use a range compensator called a bolus to conform the distal boundary of dose distribution to that of a target for proton therapy. The shape of the bolus is determined by the treatment planning program based on the broad-beam algorithm (BBA) for proton therapy. The conventional dose calculation method using the BBA[1)] has been widely used for treatment planning because of its simplicity and short calculation time. However, the calculation results using the BBA often do not agree with the measurement results for a target with large heterogeneities since it does not take into account the effect of ray mixing by multiple scattering effects of protons[2)] in materials. To demonstrate the situation, we measured dose distributions formed by the horizontal proton beam traversing a phantom with an L-shaped horizontal cross section and compared them with the calculated results using the BBA. It was obvious that the calculated results did not accurately predict the actual dose distributions.[3–6)] On the other hand, calculation by the Monte Carlo technique, which takes into account all physical interactions between particles and materials, can predict actual dose distributions more accurately. However, it requires a long calculation time, thus it is difficult to use it for routine treatment planning at present. Therefore, a number of dose calculation methods based on the pencil-beam algorithm (PBA) have been developed by Hong *et al.*[1)] and others[7–9)] to improve the accuracy of dose calculation for proton treatment planning and have with a reasonable calculation time. We modified Hong's method by considering the shape change of a depth-dose curve of a broad beam depending on the energy and by characterizing the incident broad beam by the phase space parameters at the effective source point instead of considering the source size only.

In this paper, we present a method of dose calculation based on the modified version of Hong's PBA and the predictability of dose distributions in comparison with the experimental results using an unmodulated proton beam.

*E-mail address: kohno@pmrc.tsukuba.ac.jp
†E-mail address: takada@pmrc.tsukuba.ac.jp

2. Dose Calculation Algorithm

We use a range compensator called a bolus to conform the distal end of the iso-dose curve to a distal boundary of the target in proton therapy. One of the important aspects of the proton treatment plan is to determine the shape of the bolus. However, the dose distribution of the proton beam traversing the bolus which is designed using the BBA often does not conform to the target since it ignores the angular divergence of the incident beam and the multiple scattering effect in materials. Thus refabrication of the bolus is sometimes required after measurements of dose distribution. In order to improve this situation, we have developed a more accurate dose calculation method which can be applicable to routine proton treatment planning. In this section, we describe the new dose calculation method and the conventional dose calculating method for comparison.

2.1 *Pencil-beam algorithm*

We modified a method of dose calculation based on the PBA developed by Hong *et al.*[1)] While the Hong's method expresses the proton source as an effective source with a spatial Gaussian distribution and an isotropic angular distribution, we characterize the proton source by phase space parameters at the effective source point. Using this method we can determine the behavior of proton-beam-penetrating materials such as the fine degrader, the bolus and water more accurately.

A beam of particles is conveniently described in phase space by enclosing their distribution by ellipses. The beam ellipse in the (x, θ) space is described by σ matrix. The transformation rule for such ellipses through a material of length L is given in the paper by Carli and Farley.[10)] The differential equation is

$$\frac{d\sigma}{dL} = \begin{pmatrix} 2\sigma_{12} & \sigma_{22} \\ \sigma_{22} & \dfrac{d\bar{\theta}^2}{dL} \end{pmatrix}, \tag{1}$$

$$\sqrt{\bar{\theta}^2} = \frac{14.1}{p\beta c}\sqrt{\frac{L}{L_r}}\left(1 + \frac{1}{9}\log_{10}\frac{L}{L_r}\right). \quad (2)$$

Equation (2) is termed the Highland Formula,[2] where σ_{11}, σ_{12} and σ_{22} are phase space parameters, $\sqrt{\bar{\theta}^2}$ is the rms of the distribution of the projection angle in a plane extended by the beam axis and the horizontal axis, p is the proton momentum in units of MeV/c and βc is the velocity of proton. $p\beta c$ is calculated in advance as a function of the proton range. L_r is the radiation length of the material in units of g/cm^2. The components of σ with an additional index 0 are those at the entrance of the material. The differential equations for the components σ_{22}, σ_{12} and σ_{11} have the solutions

$$\sigma_{22}(L) = \sigma_{22,0} + \int_0^L \frac{d\bar{\theta}^2}{dz}dz, \quad (3)$$

$$\sigma_{12}(L) = \sigma_{12,0} + \sigma_{22,0}L + \int_0^L (L - z)\frac{d\bar{\theta}^2}{dz}dz, \quad (4)$$

$$\sigma_{11}(L) = \sigma_{11,0} + 2\sigma_{12,0}L + \sigma_{22,0}L^2 + \int_0^L (L - z)^2\frac{d\bar{\theta}^2}{dz}dz. \quad (5)$$

The dose $F(x, y, z)$ for the point of interest at (x, y, z) by a pencil beam is given by the product of the central-axis term and the off-axis term. The central-axis term shows the measured depth-dose distribution of the broad beam. The off-axis term shows the lateral distribution at the specified depth. It is expressed by the two-dimensional Gaussian with the variance calculated by the eq. (5), taking into account the incident beam and the target conditions. The dose $F(x, y, z; (x_0, y_0))$ by a single pencil beam at an entrance position, (x_0, y_0), is given by

$$F(x, y, z; (x_0, y_0)) = \phi(x_0, y_0)DD(z; (x_0, y_0))$$
$$\frac{1}{2\pi\sigma(z; (x_0, y_0))^2}\exp\left(-\frac{(x_0 - x)^2 + (y_0 - y)^2}{2\sigma(z; (x_0, y_0))^2}\right), \quad (6)$$

where $DD(z; (x_0, y_0))$ is the depth-dose distribution of the broad beam and $\phi(x_0, y_0)$ is the measured intensity profile of the broad beam at the entrance position of the target. We can obtain the dose distribution in water by generating many pencil beams and by summing the dose distributions over (x_0, y_0).

2.2 *Broad-beam algorithm*

In the BBA,[1] the dose $F(x, y, z)$ at a given point (x, y, z) is determined by calculating the water-equivalent path length to that point and by applying the dose at the depth of the measured depth-dose curve in water. The lateral penumbra is expressed by the penumbra transmission factor considering the effective source size and the arrangement of the source, the aperture for lateral beam shaping and the patient. While the BBA predicts the dose distribution well in a relatively homogeneous target, it does not predict the dose distribution well in a target with a large lateral heterogeneity since it does not take into account the angular distribution of the incident beam and the multiple scattering effect in materials correctly. The calculation time required for the BBA is shorter than that for the PBA. Thus, the dose calculating method by the BBA has been widely used for treatment planning to date.

3. Measurement of Dose Distributions

It is well known that a dose calculation by the PBA may not accurately predict the dose distribution of protons traversing a bolus with the large heterogeneity in lateral (x)-direction since it does not model the edge scattering effect correctly. Therefore, dose distributions of protons traversing a bolus with large heterogeneity were measured in detail using a silicon semiconductor detector (SSD) for evaluation of the PBA.

Measurements were carried out using the horizontal beam line at the Proton Medical Research Center (PMRC), University of Tsukuba. Approximately monoenergetic 250 MeV protons are supplied from the KEK 500 MeV booster synchrotron through a carbon energy-degrader and a momentum-analyzing system. The incident protons were scattered by a 3-mm-thick lead plate (referred to as "the first scatterer") to obtain a laterally uniform spatial distribution. A binary range shifter of 120 mm thickness and a secondary-emission chamber (SEC) were placed between the first scatterer and the patient's table. We placed the SSD (sense volume = $2 \times 2 \times 0.05$ mm^3) in a water vessel on the patient's table to measure the dose distributions. Since the SSD has a better spatial resolution than the ionization chamber, it has been used for verification of dose distributions calculated by the present proton treatment planning system based on BBA at PMRC.

We prepared a bolus with an L-shaped horizontal cross section made of Mix-DP, which is a tissue-equivalent material for X-ray (see Fig. 1). The thicker part, $x \geq 0$, of the bolus measures 50 mm and the thinner part, $x < 0$, measures 10 mm. There is no structure in the y-direction and the height is 100 mm. It has an abrupt change of thickness in the lateral direction. This bolus shape was selected to correspond to the target with large heterogeneity in the lateral direction. The experimental arrangement is sketched in Fig. 1 (plan view).

The origin of the y-coordinate was defined at the middle of the bolus. The SSD was set at $y = 0$ in this experiment. The depth (z)-dose distributions were measured by moving the SSD in the z-direction at $x = -40$, 0 and 40 mm in water and the lateral (x)-dose distributions were measured in water at different depths ranging from $z = 160$ to $z = 210$ mm at intervals of 5 mm. We also measured the dose distribution at $z = 12$ mm, where we could observe the edge scattering effect at a shallow region.

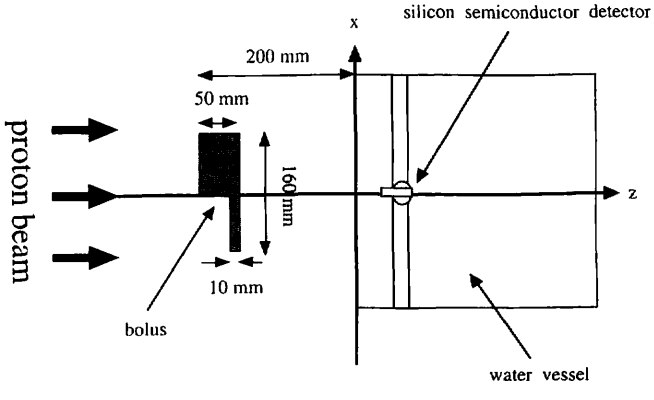

Fig. 1. Experimental arrangement for measurements of dose distributions in water (plan view).

4. Results and Discussion

The measured dose distributions are compared with the calculated ones based on the PBA and the BBA. In this calculation by the PBA, the $\sigma_{22,0}$ parameter used in the PBA was determined by measuring the beam profile passing through various materials in the beam line and a block collimator with a small circular hole, at four positions downstream from the collimator. The obtained value is 0.000078 rad^2 under the assumption that $\sigma_{11,0}$ and $\sigma_{12,0}$ are 0. Parallel pencil beams were generated with a lateral pitch of 0.5 mm at the longitudinal position of $z = -200$ mm which is the entrance surface of the bolus. The lateral pitch was selected so that a finer pitch did not produce any difference in the calculation results. Next, dose distributions in water by the group of pencil beams traversing the bolus were calculated. We normalized the relative dose so that the maximum dose (Bragg Peak) of the depth-dose distribution at $x = -40$ mm should be 100%.

Figures 2(a)–2(c) are measured depth (z)-dose distributions at $x = -40$, 0 and 40 mm along with the calculations. Figures 2(a) and 2(c) depict the region where the thickness of the bolus is uniform, as shown in Fig. 1. The depth-dose distribution by the BBA overlaps that by the PBA. Bragg peak in Fig. 2(a) is approximately at $z = 200$ mm and that in Fig. 2(c) is approximately at $z = 160$ mm. In these cases, the dose predictions by the PBA and the BBA agree well with the measured dose distributions. On the other hand, Fig. 2(b) shows the depth-dose distribution in the region where the thickness of the bolus changes abruptly. The edge effect of the bolus is evident. While calculation by PBA reproduces the measured result well, discrepancy between the measured and calculated by the BBA is significant. This is due to the fact that the dose at a given point is determined by the dose of the measured depth-dose curve at the depth determined by the water-equivalent path length up to that point based on the simple ray-tracing model in the BBA. However, the calculation based on the PBA method considers the mixing of different paths and the multiple Coulomb scattering effect in the material, which results in good agreement with the experimental results.

Figures 3(a)–3(d) depict lateral (x)-dose distributions at $z = 12$, 160, 180 and 200 mm. It is evident that calculations by the PBA can reproduce experimental data more accurately than those by the BBA. In Figs. 3(a) and 3(b) a bump and dip structure can be seen around $x = 0$. These show the edge scattering effects of the bolus region where the thickness changes abruptly. Figure 3(b) shows the large error between the results calculated by PBA and the measured results. These results indicate the limitation of the dose prediction by PBA which does not model the edge scattering effect correctly. We should consider this limitation when we apply the PBA to plan for the complex target region with a large lateral heterogeneity which occurs in the cancer of the head and neck regions. However, for most targets which have minor inhomogeneity in the lateral direction, calculations by PBA can predict dose distribution with sufficient accuracy.

Figures 4(a)–4(c) depict iso-dose distributions obtained by the measured and calculated results by PBA and those by the BBA, respectively. The isodose curves are drawn for every 10% increase of the maximum dose. Figure 4(a) is obtained by interpolating the experimental lateral-dose distributions from $z = 160$ to $z = 210$ mm every 5 mm. The white region depicts the distribution of more than 90% of the maximum dose and the black region depicts that of less than 10% dose. Figures 4(a)–4(b) show that the iso-dose distribution by the PBA agrees well with the experimental results. We compared all measurement data in the region of interest with calculations based on the PBA and found that the dose calculation by the PBA indicated a good agreement with the measurement results within the rms error of 2.3%. A part of the error arises from fluctuation of dose measurements by the SSD. The BBA has been widely used for proton dose calculation for treatment planning since it predicts dose distribution well for a target with a small lateral inhomogeneity, in a short time. However, as shown in Figs. 4(a) and 4(c), it is obvious that dose calculation by the BBA produces large dose errors for a target with large lateral inhomogeneity. Therefore, care should be taken when it is applied to such targets.

5. Conclusions

The dose distributions formed by the protons traversing an L-shaped bolus have been measured and compared with calculations based on the PBA and the BBA. While calculated

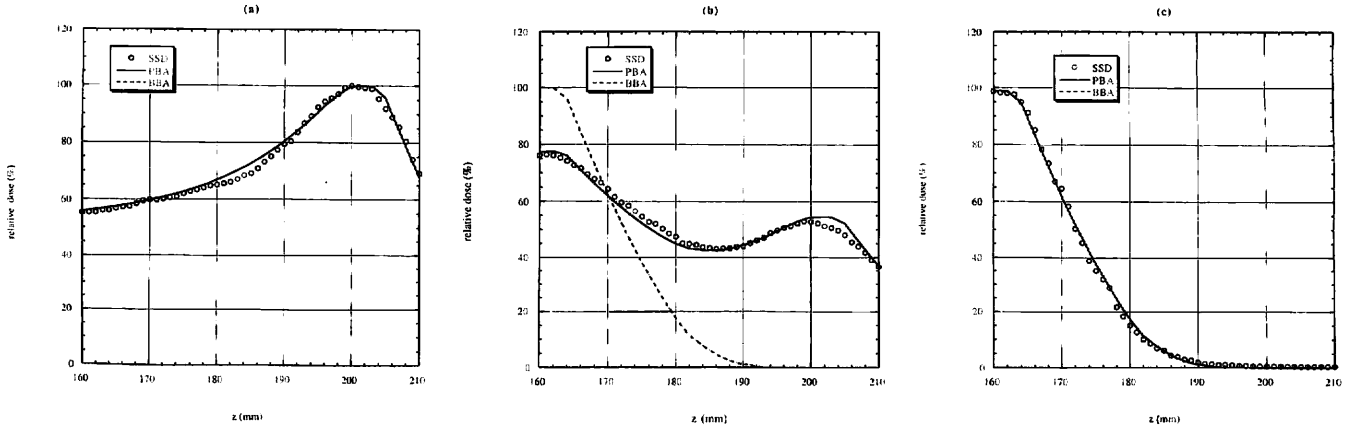

Fig. 2. Comparison of the depth-dose distributions by measurements and calculations by the PBA and those by the BBA at $x = -40$ (a), 0 (b) and 40 mm (c) in water.

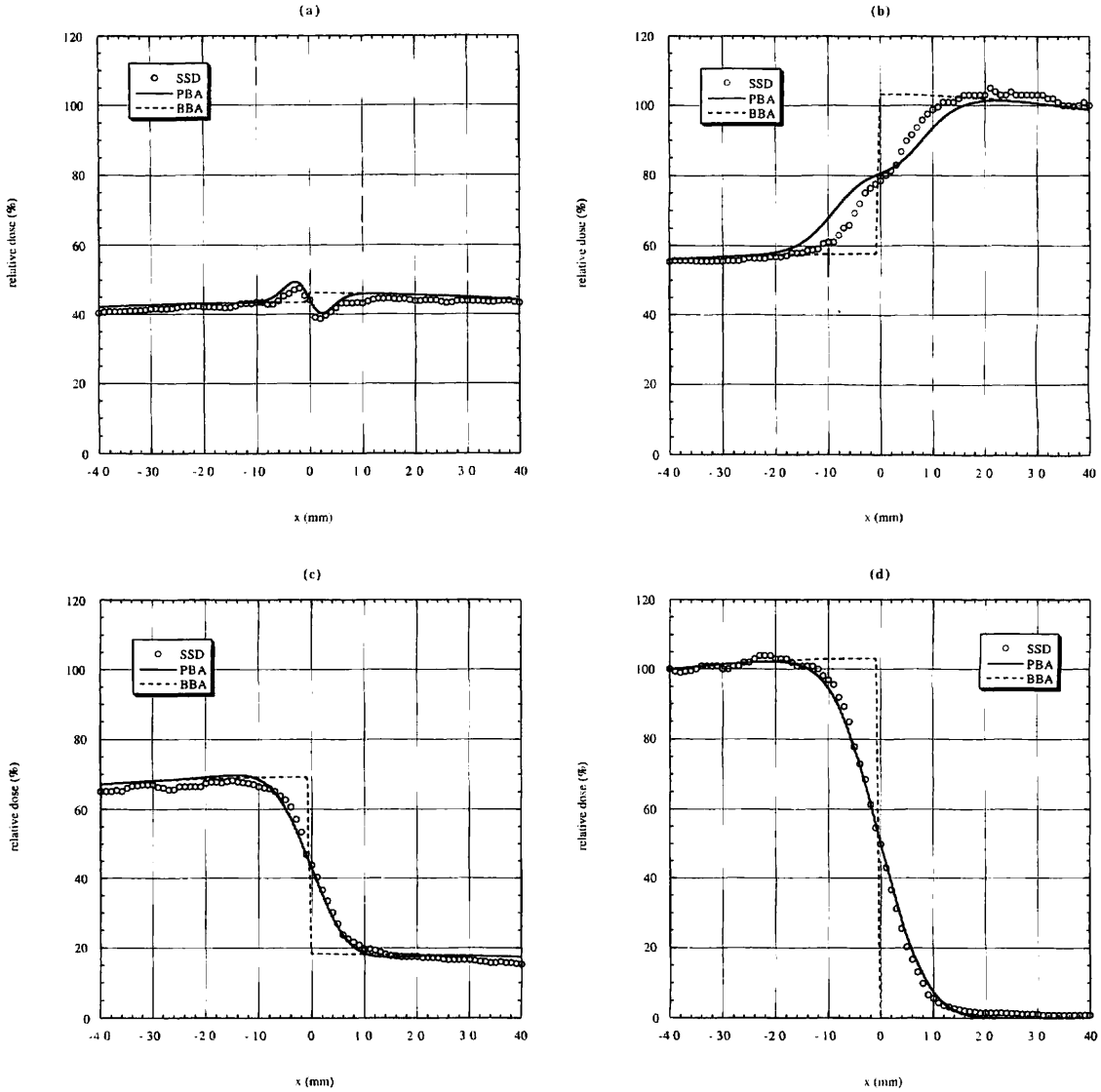

Fig. 3. Comparison of the lateral-dose distributions by measurements and calculations by the PBA and those by the BBA at $z = 12$ (a), 160 (b), 180 (c) and 200 mm (d) in water.

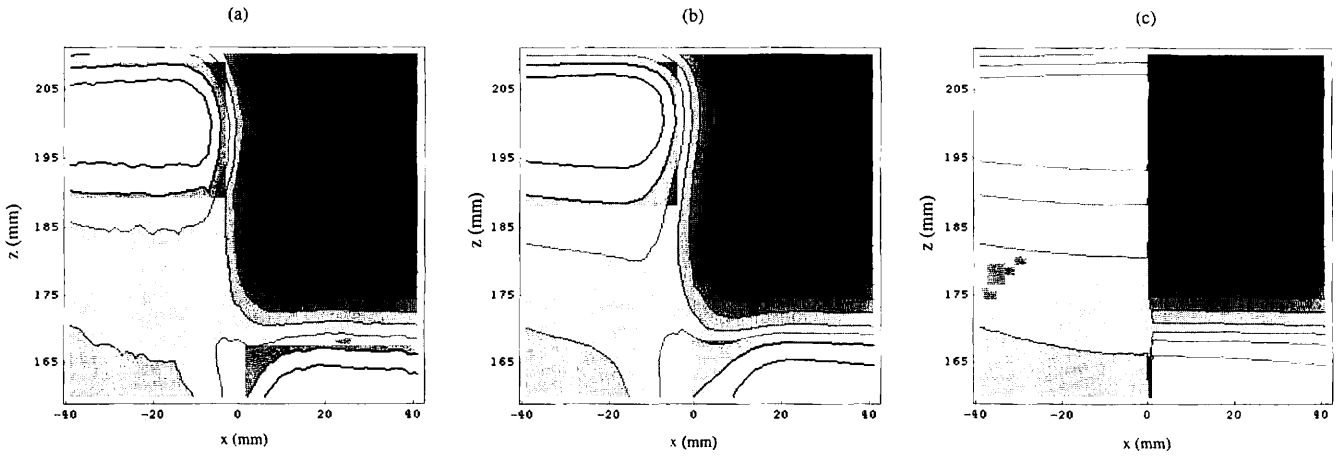

Fig. 4. Comparison of the iso-dose distributions drawn for every 10% of the maximum dose by measurements (a), calculations by the PBA (b) and those by the BBA (c) in water.

results by the PBA agree well with the measured dose distributions within the rms error of 2.3%, those by the BBA show a large discrepancy. Since the PBA does not model the edge scattering correctly, some discrepancy can be observed in the extreme case where a large lateral inhomogeneity exists. However, calculations by the PBA predict dose distribution for most practical cases with sufficient accuracy. In addition, the calculation time required by the PBA is relatively short. Therefore, it is practical to use it for the dose calculation of proton treatment planning.

1) L. Hong, M. Goitien, M. Bucciolini, R. Comiskey, B. Gottschalk, S. Rosenthal, C. Serago and M. Urie: Phys. Med. Biol. **41** (1996) 1305.
2) B. Gottschalk, A. M. Koehler, R. J. Schneider, J. M. Sisterson and M. S. Wagner: Nucl. Instrum. & Methods B **74** (1993) 467.
3) M. Goitein: Med. Phys. **5** (1978) 258.
4) M. Goitein, G. T. Y. Chen, J. Y. Ting, R. J. Schneider and J. M. Sisterson: Med. Phys. **5** (1978) 265.
5) M. Urie, M. Goitein and M. Wagner: Phys. Med. Biol. **29** (1984) 553.
6) M. Urie, M. Goitein, W. R. Holleys and G. T. Y. Chen: Phys. Med. Biol. **31** (1986) 1.
7) P. L. Petti: Med. Phys. **19** (1992) 137.
8) A. K. Carlsson, P. Andreo and A. Brahme: Phys. Med. Biol. **42** (1997) 1033.
9) B. Schaffner, E. Pedroni and A. Lomax: Phys. Med. Biol. **44** (1999) 27.
10) C. Carli and F. Farley: Eulima Feasibility Stud. Rep. (1991) February, 160.